Magnesium sulphate-silicone foam composites for thermochemical energy storage: assessment of dehydration behaviour and mechanical stability

Luigi Calabrese[1,2], Vincenza Brancato[2,*], Valeria Palomba[2] Andrea Frazzica[2], Luisa F. Cabeza[3]

[1] Department of Engineering, University of Messina, Messina, Italy

[2] CNR – ITAE – Istituto di Tecnologie Avanzate per l'Energia "Nicola Giordano", Salita S. Lucia sopra Contesse 5, Messina 98126, Italy

[3] GREiA Research Group, INSPIRES Research Centre, Universitat de Lleida, Pere de Cabrera s/n, 25001-Lleida, Spain

* Corresponding author: vincenza.brancato@itae.cnr.it

Keywords: $MgSO_4 \cdot 7H_2O$, composite foams, thermochemical energy storage, mechanical properties, TGA

Abstract

This paper assesses the mechanical stability and dehydration behaviour of a new composite material constituted by magnesium sulphate hepta-hydrate, used as filler at vary contents, and a porous silicone, used as matrix in order to evaluate its applicability in sorption thermal energy storage field. This new composite was developed to avoid the typical issues of salt hydrates such as swelling, agglomeration and corrosion issues occurring during hydration/dehydration process.

A preliminary physical-mechanical characterization, by means of morphological and calorimetric analysis, was carried out to investigate the main properties of the composite foams. The morphological characterization showed that the foam pores were homogenously distributed and well interconnected to each other. Thermo-gravimetric dehydration tests, have demonstrated that the tested samples are able to exchange efficiently water.

Static compression tests evidenced a high compression stability of the material, indicating a high flexibility of the cellular silicone structure. Furthermore, cyclic compression test was performed to evaluate the progressive loss of salt at increasing number of the cycles. After 50 cycles, a reduction of salt hydrate up to 13% was observed. This behaviour, that is potentially a critical factor in these composite structures, was studied for showing that the loss of the salt does not compromise

considerably the sorption storage performance of the filled silicone foams. Eventually, the assessment of thermo-gravimetric characteristics and mechanical stability was performed on the $MgSO_4 \cdot 7H_2O$ silicone composite foam.

1. Introduction

The use of renewable energy sources (RES), e.g. solar energy, as well as heat losses from engines and industrial waste heat represents an essential opportunity to reduce the impact of the traditional fossil sources. RES are clean, worldwide available, and inexhaustible. However, the full exploitation of RES potential requires the presence of a thermal energy storage (TES) system, in order to decouple the availability of the heat source from the user demands [1]. The technologies for TES include sensible storage [2], latent storage [3], and thermochemical storage, either with thermophysical reactions or chemical reactions [4]. Among them, thermochemical energy storage (TCS) represents a promising alternative, thanks to the high energy density, virtually zero energy losses, and the vast range of materials available for tailoring the storage to the application [5,6]. Indeed, several classes of thermochemical energy storage materials (TCMs), such as zeolites [7,8], zeotypes [9], and salt hydrates [10–12], have been investigated. A complete review of studies on materials for sorption storage applications can be found in [13,14]. A clear outcome of the vast majority of studies in literature is the outstanding energy density of reversible reactions involving salts, such as hy/dehydration reactions. Indeed, their theoretical storage capacity in the range of temperatures under 100°C can reach 3 GJ/m^3[10]. Nonetheless, their practical application still needs research efforts, because different problems arise when these materials are used in a storage system. Among them, agglomeration and swelling phenomena, that limit the vapour diffusion and induce degradation after cycling [15] are the most critical. At the same time, low thermal conductivity of the materials also represents a serious drawback in the use of salt hydrates in a storage system. In order to prevent such an issue, dispersion of the salt in a matrix has been proposed in literature. Among the available matrices, expanded graphite and porous adsorbent materials (zeolite, silica gels and activated carbons) have been studied [16], as well as carbon-based foams [17,18]. Hongois et al. [19] and Whiting et al. [20] used different type of zeolites for the wet impregnation of $MgSO_4$ salt into the ceramic container. Analogously, Posern et al. [21] used attapulgite powders as matrices for the impregnation on a mixture of $MgSO_4$ and $MgCl_2$. Jabbari-Hichri et al. [22] studied $CaCl_2$ with three different matrices: silica gel, alumina, and bentonite showing that the best performance in terms of stored/released heat and water sorption capacity was obtained with the silica gel impregnated composite. More recently, Xu et al. [23] studied the hydration behaviour of $MgSO_4$ embedded into zeolites for open sorption heat storage in a prototype storage. The results showed that the prepared zeolite-$MgSO_4$ composites had larger hydration ability than pure zeolites, and zeolite 13X-$MgSO_4$ showed the best performance. Up to five discharges were realised, without noticing any performance loss, thus concluding that the cyclability of the material can be, in a first approximation, considered satisfactory. Xu et al. [24] evaluated the application for the heat storage of $MgSO_4$-13 X zeolite and

$MgSO_4$-activated alumina composites through TGA-DSC. The results showed that the impregnated $MgSO_4$ improves the overall TES performances of both 13X zeolite and activated alumina, with 13X zeolite based composites preferable for open sorption storage applications, and activated alumina ones for closed sorption. Mehrabadi and Farid [25] evaluated the energy density and dehydration behaviour of five different salts; $Al_2(SO_4)_3 \cdot 18H_2O$, $MgSO_4 \cdot 7H_2O$, $CaCl_2 \cdot 6H_2O$, $MgCl_2 \cdot 6H_2O$, and $SrCl_2 \cdot 6H_2O$ using two porous matrices, expanded clay and pumice. The results showed that $SrCl_2 \cdot 6H_2O$ has the highest energy density and lowest dehydration temperature. Up to 29 kWh/m^3 and 7.3 kWh/m^3 energy can be stored using expanded clay-$SrCl_2$ (40 wt.%) and pumice-$SrCl_2$ (14 wt.%), respectively. However, cyclability behaviour was poor, since after less than 10 cycles the performance dropped sharply.

It is then possible to conclude that, generally, composites present enhanced properties with respect to the pure salts, in terms of thermo-physical properties and kinetic ones, allowing also to increase the performance at reactor level [26]. However, the major limit of the investigated matrices is their rigid structure, which may suffer of long-term stability issues, due to the forces induced by the salt solution expansion during the hydration phase. Furthermore, the salt is usually confined into open pores, which are not able to keep the solution in case of oversaturation, causing a degradation of the composite itself [24]. In this regard, polymeric foams can overcome most of the reported issues, since they present a flexible structure, allowing for the safe volume expansion during the hydration phase. Furthermore, some polymeric foams are permeable towards water vapour, allowing the vapour reacting also with salt confined inside closed porosity [27].

In such a context, recently, this innovative concept was proposed for thermal energy storage applications by Brancato et al. [28], employing a composite $MgSO_4$ filled silicone macro-porous foam. The elasticity and flexibility of this foam [29], allowing the expansion of the salt hydrate volume during its hydration process, are able to enhance the mechanical stability of the composite material,. Furthermore, the chosen matrix has an effective water vapour permeability, thus guaranteeing suitable hydration/dehydration reaction phenomena in the $MgSO_4$ hosted salt. The preliminary thermo-physical and structural characterisations confirmed the reliability of the proposed solution [30].

The present work further develops the proposed concepts, by analysing the mechanical properties and dehydration performance of the $MgSO_4 \cdot 7H_2O$ – silicone foam composites. The analysis of the mechanical stability seems to be highly necessary due to the salt loss observed in [28]. Indeed, the loss of the hydrated salt could strongly compromise the thermochemical performances of the composite foams, and thus their storage capacity. With the aim to verify the mechanical stability of

the composites, static and cyclic compressive tests were carried out, showing that the loss of the salt does not compromise considerably the sorption storage performance of the filled silicone foams.

2. Materials and methods

The polymeric foams, based on a mixture of poly(methylhydrosiloxane) and a silanol terminated polydimethylsiloxane filled with different percentages of the salt hydrate, were obtained following the procedure shown in [30]. In particular, a mixture constituted by poly(methylhydrosiloxane) $(CH_3(H)SiO)_n$ (PMHS) as monomer and a silanol terminated polydimethylsiloxane (PDMS) as hardner with bis(2-ethylhexanoate)tin as catalyst (all supplied by Gelest Inc., Morrisville, USA) was employed. The selected silicones were chosen as matrix in the composite foam thanks to their high water vapour permeability. Therefore, the polymeric matrix does not affect the water vapour diffusion, insuring the hydration/dehydration phenomena during the real operating conditions.

The $MgSO_4 \cdot 7H_2O$ salt hydrated was dispersed, under vigorous mixing, in different percentages (ranging from 40-70 wt.%) in the siloxane matrix up to reach a homogeneous slurry. Then the foaming process was performed placing the slurry in a cylindrical mould under controlled temperature (60°C for 24 h). In Figure 1, the procedure for the salt-silicone foam samples preparation is reported.

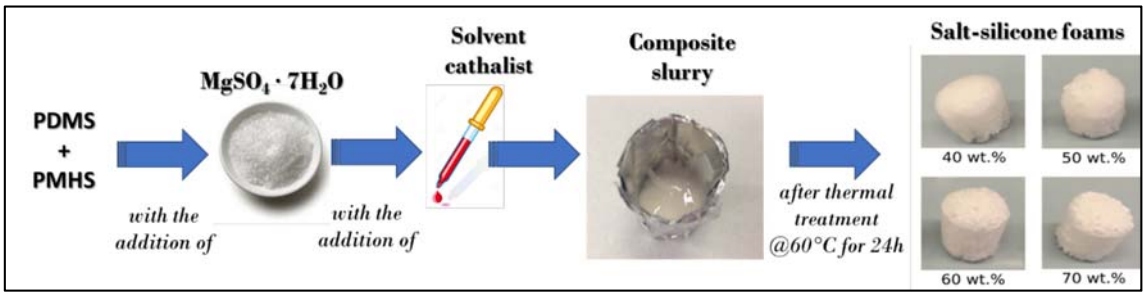

Figure 1: Scheme of the preparation steps of the salt-silicone foams

The reaction between the hydroxyl and hydride functional groups of PDMS and PMHS respectively, forms a siloxane Si-O-Si bridge that progressively led to a tri-dimensional rubber-like silicone network. Gaseous volatile hydrogen is also obtained as reaction product and acts as foaming agent.
As indicated from the authors, the chosen polymeric matrix present high permeability to the water vapour, in order not to hinder the water vapour diffusion during the working procedure [31] [32]. The obtained foam samples are codified as "F_Mg" plus a number that indicates the amount of the salt added to the polymer host (e.g. F_Mg40 designates the foam filled with 40 wt.% $MgSO_4 \cdot 7H_2O$). In Figure 2 the obtained foam samples with salt content varying from 40 wt.% up to 70 wt.% are presented.

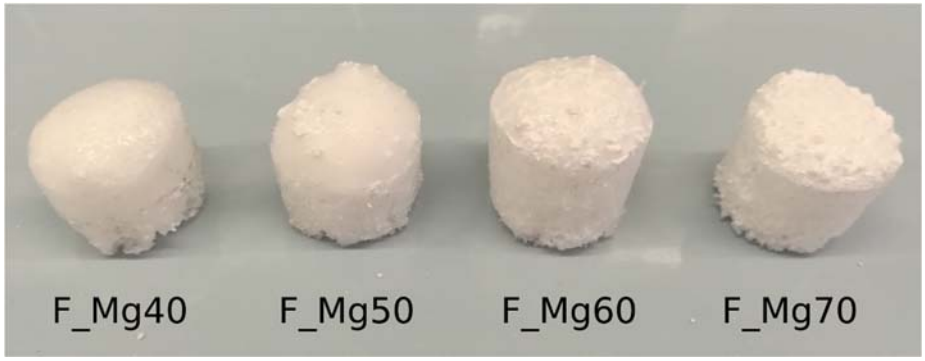

Figure 2: Prepared composite foam samples with different MgSO4·7H2O content from 40 wt.% to 70 wt.%

The polymeric composite foams were characterized by means of thermo-gravimetric analysis (TGA) performed by an adapted instrument, Labsys Evo manufactured by SETARAM [33]. The measurements were performed according to the following procedure: few milligrams of sample were weighed by a microbalance and placed inside the measurement apparatus. The degassing was performed at room temperature and up to a pressure of $1*10^{-3}$ mbar. The water vapour, produced by an evaporator at a temperature of 20 °C, was then admitted into the measuring chamber in order to create an environment saturated by water vapour at 23.4 mbar pressure. A heating ramp of 5 ºC/min from room temperature up to 150°C was performed to evaluate the evolution of the dehydration process of the foams, using test conditions mimicking the working ones.

Morphological analyses of the cross section of foams were obtained at 50x magnification using a 3D optical digital microscope (Hirox HK-8700).

Compression tests were performed on prismatic shaped samples, with dimension 10x10x10 mm^3, cut out from the moulded cylinder foams. Parallelism of top and bottom surfaces was checked by using a 3D optical digital microscope. Specimens with parallelism tolerance higher than 3° were discarded. Static compression tests were performed by using a universal testing machine (2.5kN Zwick Line) equipped with a 2.5 kN load–cell. Crosshead speed was 1.0 mm/min. Three replicas for each batch were carried out.

3. Results and Discussion

3.1 Morphological analysis

The cross-section images at 50x magnification, obtained by a 3D optical microscope, are shown in Figure 3. For the sake of clarity, the photos are taken for samples F_Mg40 and F_Mg60. Both the images are captured along the foaming direction, in order to evaluate how the salt content modifies the foaming process.

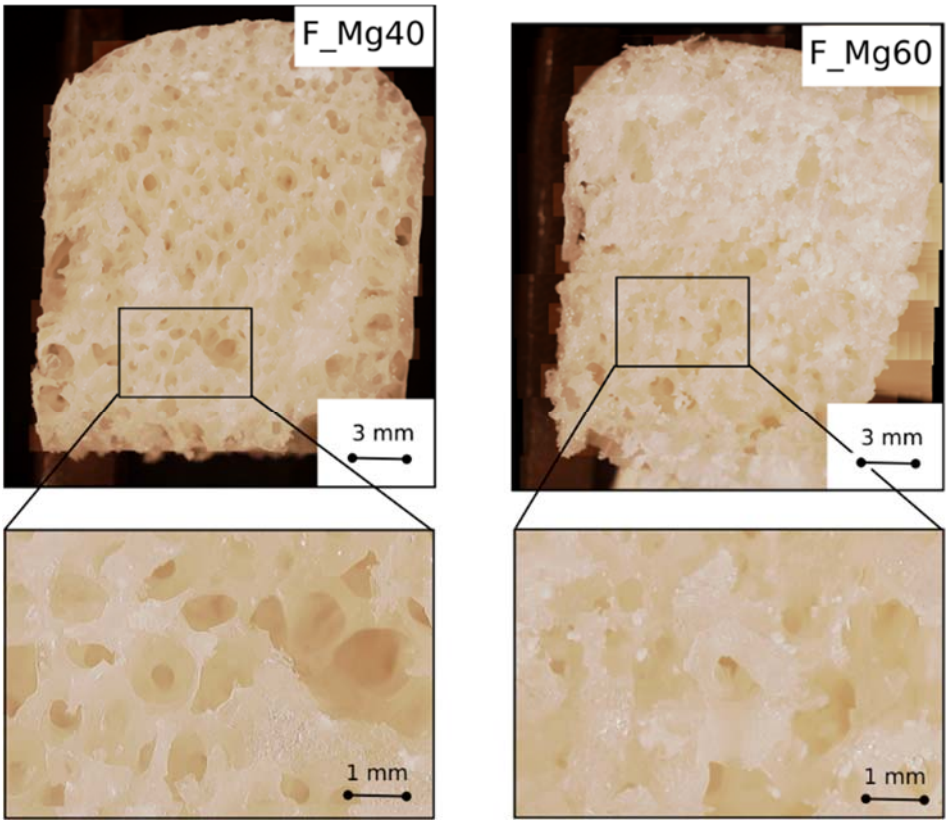

Figure 3: 3D optical images of sample: F_Mg40 and F_Mg60

Both samples show a mixed open/closed cell structure, whit bubbles homogenously distributed and well interconnected to each other. It is possible to see that higher amount of salt hydrate (60 wt.%) slightly reduces the foamability of the polymeric materials and the proper inclusion of salt grains within the matrix. Actually, the magnification of the pore structure demonstrates that salt grains are deeply confined inside the polymeric foam in the sample F_Mg40, while in the sample F_Mg60 there are numerous grains on the surface. Indeed, differently from what was observed for the composites produced with the same matrix and zeolite [31], the use of salt hydrate does not lead to the formation of chemical bonds; the salt is only confined and mechanically constrained inside the porous structure. By evaluating a detail of the cross-section images, the composite morphology and cell microstructure can be better analysed. The cell structure is well defined and interconnected. During the foaming stage, the bubbles interact and coalesce generating macro- and micro-channels thus offering a very wide and tree-dimensional contiguous paths network.

For large salt hydrate content in the foam, the bubble coalescence phenomenon is slightly hindered. If a high amount of salt hydrate is added in the foam, a significant increase on the viscosity value of the salt-matrix composite slurry can be observed. This reduces the chemical and physical foaming process and subsequently limits the bubbles coalescence during the foaming phase [34]. Consequently, small size bubbles were obtained. Despite this, the foam is still porous and characterized by a well-shaped cell structure. A tree-dimensional network of contiguous paths for vapour diffusion can be observed both for low and high salt content foam.

In any case, the presence of a homogenous porous structure in the cross section, evidenced also with the other salt percentages [30], permits an efficient water vapour exchange between the inner and the external part of the foams.

Scanning Electron Microscopy (SEM) analysis was carried out to better highlight salt distribution in the silicone foam. Figure 4 shows the micrograph of F_Mg40 sample. In the picture punctual EDS results on pure silicone matrix (P1 point) and salt filler (P2 point) are also reported.

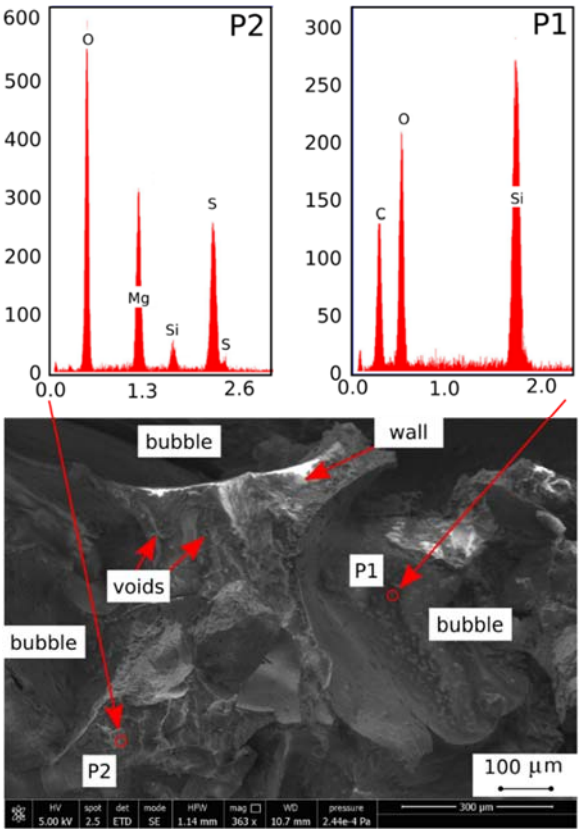

Figure 4: Micrograph and EDS spectra of F_Mg40 sample

The composite foam microstructure is constituted by salt hydrate grains well embedded in the silicone matrix. Although no chemical interaction between salt and matrix occurred, the salt hydrate is

effectively mixed and adherent to the silicone foamed binder. The cross section of the cell wall is homogenous without evident defects or cracks. Few voids can be evidenced in the bulk, probably ascribed to physical or chemical foaming phenomena in the foam [31]. Furthermore, thanks to the high filmogeneity of the polymer matrix sometimes the salt hydrate grains are entirely encapsulated in the structure reducing the risk of their removal during hydrothermal cycling or during handling. This is confirmed by EDS spectra, where the characteristic silicone peaks are still present on the grain of salt hydrate spectrum (EDS Spectrum of P2 point).

3.2 Dehydration analysis

Thermo-gravimetric dehydration analyses under water vapour pressure of 23.4 mbar were carried out in order to evaluate the dehydration evolution of the synthetized composites foam-salt at increasing temperature. The results of the tests are shown in **Figure 5**. Prior to the evaluation of composites, the basic components (i.e. salt hydrate and silicone foam) were tested separately in order to evaluate their behaviour. In accordance with the literature results reported in [35][36], the pure $MgSO_4$ salt, tested as reference, lost six molecules of water that corresponds to a mass loss of about 45% at 150°C. Instead, the unfilled foam, not reported in figure, evidenced a negligible weight loss in the range of 30-150°C. Therefore, considering the inert action offered by PDMS matrix, weight loss trend observed for all composite silicone foam can be ascribed to dehydration process of magnesium hydrate salt filler.

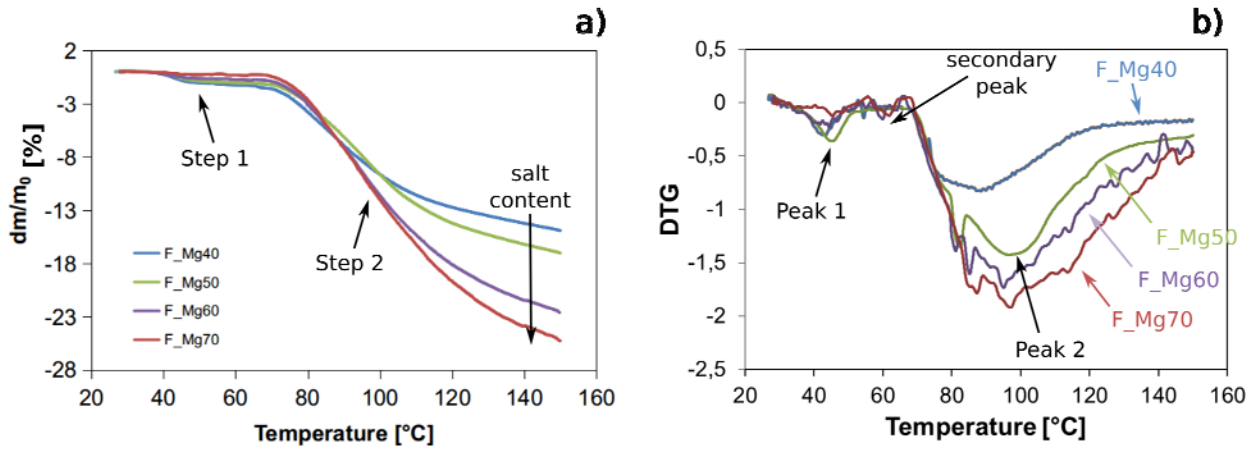

Figure 5: Thermo-gravimetric dehydration curves: (a) weight loss, dm/m_0; (b) first derivate of the weight loss, DTG

Thermo-gravimetric dehydration results for the composite, shown in **Figure 5**a, highlight that the maximum percentage of dehydration at 150°C is obtained increasing the salt content within the matrix. Indeed, F_Mg70 foam shows a maximum reduction equal to 25.31%. This indicates that the salt inside the foam is able to effectively exchange water molecules during the dehydration process.

This result confirms that the matrix does not obstruct the evaporation process, thanks to its high permeability to the water vapour. Therefore, based on common weight loss evolution, the dehydration phenomena of the pure salt and the F_Mg70 foam could be considered qualitatively compatible. Similarly, the F_Mg40 foam shows a weight loss percentage of 14.92%, essentially due to the lower salt content in this batch.

Both for high and low salt content, it is important to point out that the weight loss occurs in two different steps, the first one at about 40-45°C and the second at 90°C. The first weight loss is less significant because it is associated to the evaporation of a few water molecules, whereas the second step is the most important because it is related to the loss of the majority of the water molecules.

In addition, **Figure 5**a reveals that the weight loss is not proportional to the salt content inside the matrix. Probably, this trend could be justified considering that a localised loss of salt hydrate filler takes place during the handling of the composite samples. Actually, F_Mg70 and F_Mg40 showed an effective dehydration performance compatible to their filler content, otherwise F_Mg70 exhibits a lower weight loss (25.31%) with respect to F_Mg40 (14.92%). Indeed, the theoretical values should be 31.5% for F_Mg70 and 18% for F_Mg40. This behaviour could be explained considering that the lower is the salt content, the better is the embedding process inside the matrix, while high amounts of salt do not guarantee such a stable integration of the filler inside the matrix.

By analysing, the trend of the DTG curves (**Figure 5**b), all composite foams show two peaks of the first derivative that can be related to two distinct weight loss transitions (as described above). Peak 1 takes place at lower temperatures (40-45°C range) where a small mass reduction can be identified, while peak 2 appears at higher temperature, close to 90°C. Anyway, it seems that the first peak becomes significant at lower salt content within the foams. The foams with the high salt content do not clearly show this transition. This could be attributed to the bigger barrier action offered by the silicone matrix on F_Mg40 and F_Mg50 samples. This could generate the request of higher energy contribution to favour the removal of the first molecule of water.

In addition, the main peak of foams at lower salt content is shifted towards lower temperatures with respect to the peak of foams with higher salt amounts. This trend is not confirmed in F_Mg70 sample, where a wide and depressed peak is observed. Instead, for this sample a clearly evident secondary peak at about 60°C takes place. A similar consideration can be observed for F_Mg60 sample. This different sensitivity to dehydration process in this range of temperature for composite foams at high salt hydrate content is still not clear. Considering the minimum (40 wt.%) and the maximum salt content (70 wt.%), a plausible explanation of this phenomenon could be that the thickness of silicone foam, in the F_Mg40 is higher in comparison to the thickness of silicone foam in F_Mg70. Therefore,

the grains of the salt are deeper embedded in the matrix inducing a modification on the dehydration process. However, thanks to the interconnected macroporous structure, the composite silicone foam allows an efficient flow of water molecules from the inside to the outside during the dehydration phase. Consequently, the cells interconnection and microstructure of the foam represent a relevant factor to better understand the phenomena that oversee the hydration and dehydration processes of the functional filler located inside the foam. In this context, the digital optical microscopy technique was chosen as a valid support to investigate the foam morphology, where a tridimensional network of contiguous paths for vapour diffusion were observed both for low and high salt content foam. These preferential paths could play a fundamental role in the water vapour flow during the salt hydration/dehydration phase, making this material, an effective system for sorption thermal energy storage application.

A scheme of a possible water vapour diffusion mechanism that could take place in the composite foams was proposed according to the experimental characterisation outcomes. Indeed, the knowledge of this aspect is extremely important in order to predict the behaviour of a real thermochemical storage system, considering that the water vapour diffusion inside the matrix affects also its stability.

Figure 6 schematically depicts the vapour diffusion inside the foam. The cellular structure of the foam is mainly characterised by large bubbles interconnected (point A in Figure 6 left) that represents a preferential path for vapour way. Moreover, in consideration of the low thickness of the cell walls, also neighbouring bubbles can effectively contribute to a rapid vapour flow (point B Figure 6, left). In this area, the salt hydrate embedded in the silicon matrix can easily interact with the vapour phase, undergoing hydration/dehydration phases. Not all of the salt hydrate is able to provide a rapid hydration/dehydration process. The crystals of salt, shielded by thick matrix layer, could be inactive (point C in Figure 6, left). The salt hydration/dehydration can be also allowed by secondary flow lines (point D in Figure 6 left) induced by salt hydrate domains just in proximity of bubble border.

Therefore, based on Figure 6 right, the scheme of possible vapour flow pathways can be summed up as follows: the salt hydrated can be considered as a vapour sink and red arrows are the vapour flow paths. The vapour flow takes place mainly by bubbles interconnected paths in the foam and partially by diffusion through PDMS cell walls.

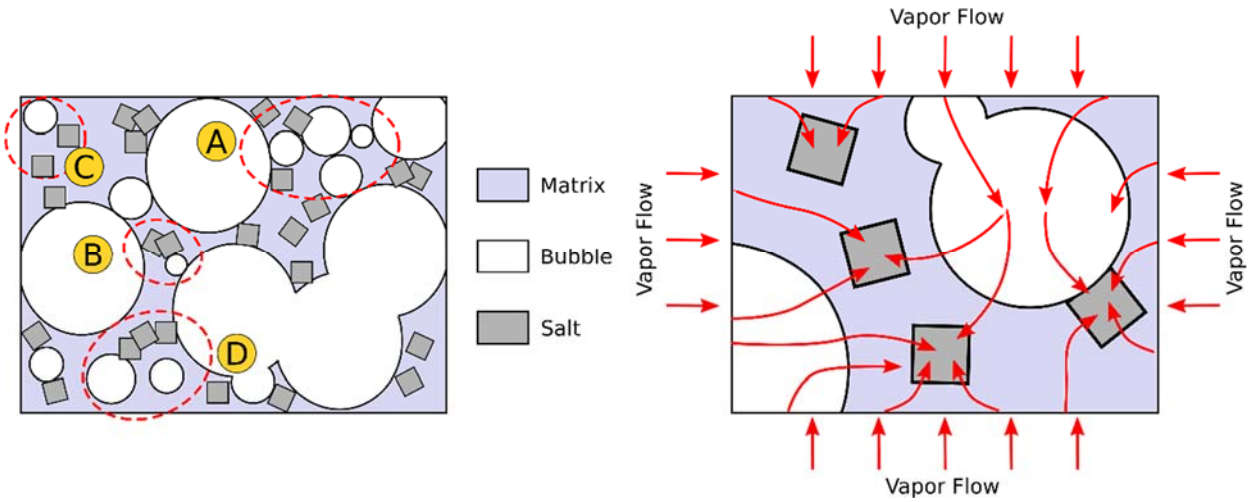

Figure 6: Water vapour diffusion schema inside the foam (left and right)

3.3 Compression test

The choice of the PDMS matrix also plays an important role for guaranteeing the mechanical stability of the composite under hydration/dehydration cycles.

Indeed, when the salt dehydrates, a volume reduction proportional to the number of the lost water molecules occurs. Consequently, as shown in Figure 7, at the matrix/filler interface, tensile or compression radial stresses take place, depending on dehydration or hydration phenomenon, respectively. A flexible matrix, if compared to a brittle one, allows greater local deformation, favouring an easier relaxation of internal forces and thus reducing the risk of damage and the loss of efficiency. In order to evaluate the deformation capabilities of foamed structure some static compression tests were carried out by using a universal testing machine.

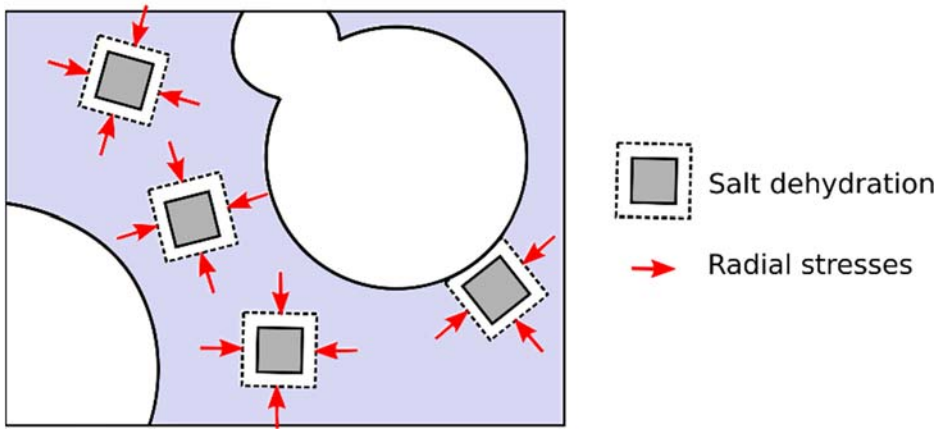

Figure 7: Scheme of internal stresses induced by volume reduction of salt dehydration compression test for unfilled silicone foam

Figure 8 reports the results for the compression test on F_Mg40 reference sample. Three different regimes can be identified: an initial elastic regime, followed by a very large plateau that corresponds to the bubbles collapse. This occurs at a low stress level (about 5-20 Pa) indicating a soft mechanical behaviour of the foam. This stage is full reversible thanks to the elastic behaviour of the foam. If the load is released the sample recovery its initial shape, without evidence of residual strain. At about 75% of strain, transition densification regime occurs, which corresponds to a significant deformation. The results confirm the high flexibility of the silicone porous structure, which is able to bear reversibly high-localized deformations.

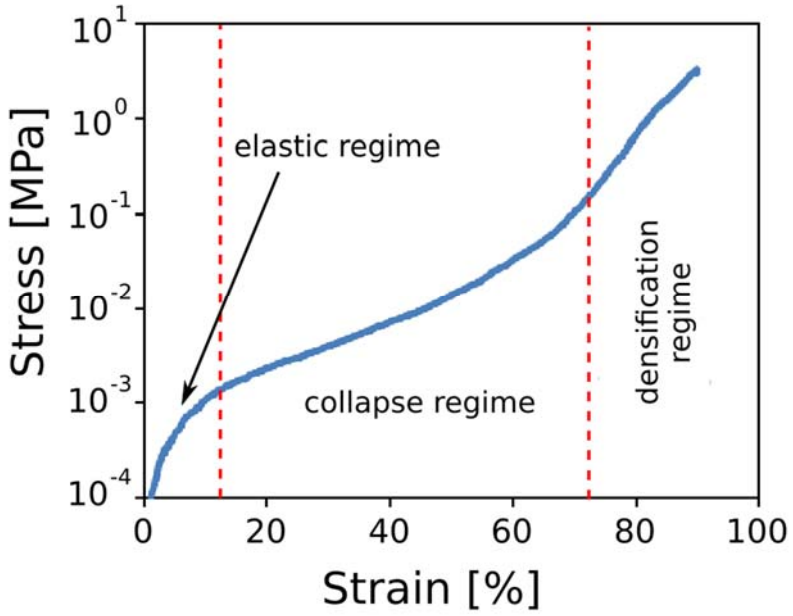

Figure 8: Stress-strain compression curve for F_Mg40 silicone foam

Figure 9 compares the compression curve for all composite foams. A progressive increase in strength and stiffness can be highlighted at increasing $MgSO_4$ salt hydrate content in the composite. Indeed, the observed mechanical behaviour up to a salt content of 50 wt.% is similar. Instead, above this threshold a slight modification of the stress-strain relationship can be evidenced: the stress in the elastic regime and densification regime increases. This indicates that that the composite foams at high salt content are characterised by a higher elastic modulus and stiffness and enhanced mechanical strength. However, the strain at which transition from collapse to densification regime is quite similar for all the samples (almost near to strain 75%). These results indicate that all composite foams have good mechanical stability and elasticity, compatible to hydration/dehydration cycles occurring in TES applications.

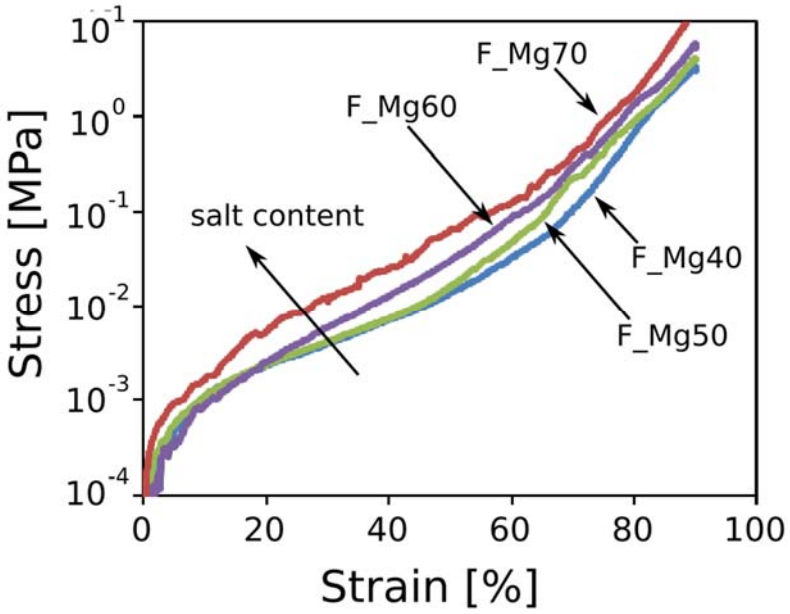

Figure 9: Stress-strain compression curve at increasing filler content for composite silicone foam

With the aim of verifying the reliability of the dehydration performance, thermo-gravimetric analysis was carried out on the salt filled composite foam after a mechanical cyclic aging up to 50 cycles, considering a threshold strain value for each cycle of 50%. The mechanical stability of the foam is required in order that the foam is able to suffer the internal stresses induced by the hydration and dehydration cycles. The foam has an elastic behaviour with a high flexibility, and this makes it potentially suitable for TES applications. Although, coupled to mechanical stability it is important to evidence the effective stability of the salt in the siloxane matrix, during aging cycles. In Figure 10, the comparison of weight loss in dehydration process for un-aged and mechanically aged F_Mg60, as reference, is reported. The weight loss becomes progressively lower for aged sample, indicating that the salt contribute on the dehydration capability of the foam is less effective. In particular, at 150°C a reduction of about 19 wt.% can be highlighted. This behaviour can be ascribed to a loss of salt filler during the mechanical cycles. This indicates that not all the salt is homogenously embedded in the silicone matrix, thus favouring local removal when the mechanical deformation takes place in the cellular structure of the foams.

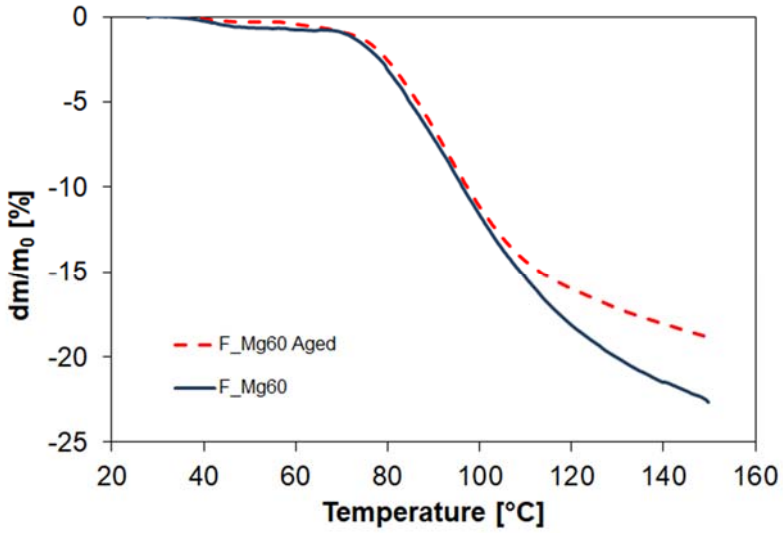

Figure 10: Thermo-gravimetric dehydration curves of mechanically aged and unaged F_Mg60 foam

In order to better relate the effect of mechanical aging on the hydration/dehydration performance of the foams, the extent of salt reduction was calculated. In particular, Table 1 shows the salt content in all the tested samples, before and after mechanical cycling. Nominal and actual salt contents, according to [28] are defined as the attended and experimentally verified salt content according to TGA measurements. In order to identify the salt loss, the weight of each fresh and aged sample was recorded. Assuming that the polymeric part does not undergo any weight change, the residual salt content was calculated as ratio between the initial and final mass of salt.

Table 1: Evaluation of salt content in composite foams before and after mechanical cycling

	$MgSO_4$		Foam		MgSO4			
CODE	Nominal salt content [%]	Actual salt content [%]	Initial weight [g]	Final weight [g]	Initial weight [g]	Final weight [g]	Residual Salt [%]	Salt reduction [%]
F_Mg40	40%	37.2%	0.47	0.44	0.173	0.149	33.7%	3.4%
F_Mg50	50%	41.1%	0.49	0.45	0.201	0.161	35.8%	5.2%
F_Mg60	60%	56.7%	0.56	0.45	0.318	0.211	46.5%	10.2%
F_Mg70	70%	58.4%	0.63	0.48	0.366	0.215	45.2%	13.2%

The results evidence a progressive increase in the amount of salt lost at increasing filler content in the foams. For F_Mg40 and F_Mg50 the salt reduction is low, since a reduction of 3.4% and 5.2% was measured, respectively. Instead, a significant reduction of salt content (13.2%) was observed for F_Mg70, indicating that the non-optimal cohesion between the constituents can have a detrimental effect on the dehydration performance of the material.


(a)

(b)

Figure 11: 3D optical images of F_Mg60 sample before and after compressive ageing

Figure 11 shows optical images of F_Mg60 foam, used as reference, before and after 50 cyclic compression test. The amount of salt hydrate in the composite foam after the mechanical aging is clearly reduced. Mainly some portions of salt, located in the foam bubbles, are detached from it and removed. As previously discussed, this salt reduction is in the range of 10% for composite foam with 60% of filler. However, after mechanical aging (**Figure 11**b) the foam morphology is quite similar to the fresh one (**Figure 11**a). From a structural point of view, the silicone foam is still mechanically stable. No evidence of cracks can be highlighted. The cell walls are well defined and the interconnected cellular structure can be still identified, thus inducing the effective water vapour diffusion phenomena in preferential pathways.

Nevertheless, the thermochemical and mechanical stability of the composite foam represents a relevant issue that needs to be investigated. Indeed, loss of the performance of the composite foams during time could be a limiting factor for its real scale applicability. Therefore, further studies will be employed to better evaluate the durability and stability of the foams in terms of hydration/dehydration process related to mechanical and micro-structural properties of the material, in order to effectively define the suitable conditions for its use in TES systems. Furthermore, the hydrothermal stability can provide tangible information on the applicability of the composite material for TES applications under real stress conditions. In this context, an activity aimed to assess the hydrothermal stability of the foam in dehydration/hydration cycles is developing.

4. Conclusions

An innovative $MgSO_4 \cdot 7H_2O$ filled silicone composite foam was evaluated for sorption thermal energy storage applications. In particular, in this work, dehydration process of the composite foamed material at varying filler content (40-70 wt.% salt content) was investigated.

1. Morphological analysis evidenced that the foam is constituted by an interconnected open/closed porous structure strictly influenced by salt filler content. At increasing filler content, a progressive increase in composite material density and reduction in bubble size was found.
2. The thermo-gravimetric analysis, performed for all the salt-silicone foams, showed good dehydration performances, further confirming that the silicone matrix does not hinder the water vapour diffusion.
3. Mechanical characterization, by static compression test, indicated good stability of the silicone cellular structure also at large deformations. However, a progressive loss of salt can be identified at increasing compression cycles. After 50 cycles a reduction up to 13% was observed. This behaviour could be ascribed to the hydrophobic behaviour of the siloxane matrix that limits the interaction between the matrix and the salt hydrate filler. These aspects were identified as potentially critical factors that needs to be better assessed -and eventually addressed- in order to obtain an effective durability and high water exchange of these structures.

Nonetheless, the results can be considered promising and therefore the system, if accurately tailored, represents an interesting configuration for TES. In particular, in order to improve the cohesion between the composite materials constituents, siloxane matrix with lower hydrophobic behaviour will be investigated. This could be a potentially effective approach to increase the interfacial interaction between the hydrate filler and the silicone matrix allowing a more effective and stable composite foam under cyclic aging.

Acknowledgements

The work was partially funded by the Spanish government (ENE2015-64117-C5-1-R (MINECO/FEDER)). The authors would like to thank the Catalan Government for the quality accreditation given to their research group (2017 SGR 1537). GREiA is certified agent TECNIO in the category of technology developers from the Government of Catalonia. This work is partially supported by ICREA under the ICREA Academia programme.

References

[1] D. Aydin, S.P. Casey, S. Riffat, The latest advancements on thermochemical heat storage systems, Renew. Sustain. Energy Rev. 41 (2015) 356–367. doi:10.1016/j.rser.2014.08.054.

[2] A.I. Fernandez, M. Martínez, M. Segarra, I. Martorell, L.F. Cabeza, Selection of materials with potential in sensible thermal energy storage, Sol. Energy Mater. Sol. Cells. 94 (2010) 1723–1729. doi:10.1016/J.SOLMAT.2010.05.035.

[3] K. Kant, A. Shukla, A. Sharma, Advancement in phase change materials for thermal energy storage applications, Sol. Energy Mater. Sol. Cells. 172 (2017) 82–92. doi:10.1016/J.SOLMAT.2017.07.023.

[4] A. Frazzica, L.F. Cabeza, eds., Recent Advancements in Materials and Systems for Thermal Energy Storage, Springer International Publishing, Cham, 2019. doi:10.1007/978-3-319-96640-3.

[5] J. Cot-Gores, A. Castell, L.F. Cabeza, Thermochemical energy storage and conversion: A-state-of-the-art review of the experimental research under practical conditions, Renew. Sustain. Energy Rev. 16 (2012) 5207–5224. doi:10.1016/j.rser.2012.04.007.

[6] S. Vasta, V. Brancato, D. La Rosa, V. Palomba, G. Restuccia, A. Sapienza, A. Frazzica, Adsorption heat storage: State-of-the-art and future perspectives, Nanomaterials. 8 (2018). doi:10.3390/nano8070522.

[7] J. Jänchen, D. Ackermann, H. Stach, W. Brösicke, Studies of the water adsorption on Zeolites and modified mesoporous materials for seasonal storage of solar heat, Sol. Energy. 76 (2004) 339–344. doi:10.1016/J.SOLENER.2003.07.036.

[8] D. Alby, F. Salles, J. Fullenwarth, J. Zajac, On the use of metal cation-exchanged zeolites in sorption thermochemical storage: Some practical aspects in reference to the mechanism of water vapor adsorption, Sol. Energy Mater. Sol. Cells. (2017). doi:10.1016/j.solmat.2017.11.020.

[9] N. Yu, R.Z. Wang, L.W. Wang, Sorption thermal storage for solar energy, Prog. Energy Combust. Sci. 39 (2013) 489–514. doi:10.1016/j.pecs.2013.05.004.

[10] P.A.J. Donkers, L.C. Sogutoglu, H.P. Huinink, H.R. Fischer, O.C.G. Adan, A review of salt hydrates for seasonal heat storage in domestic applications, Appl. Energy. 199 (2017) 45–68. doi:https://doi.org/10.1016/j.apenergy.2017.04.080.

[11] H.U. Rammelberg, T. Osterland, B. Priehs, O. Opel, W.K.L. Ruck, Thermochemical heat storage materials – Performance of mixed salt hydrates, Sol. Energy. 136 (2016) 571–589. doi:10.1016/J.SOLENER.2016.07.016.

[12] A. Gutierrez, S. Ushak, V. Mamani, P. Vargas, C. Barreneche, L.F. Cabeza, M. Grágeda, Characterization of wastes based on inorganic double salt hydrates as potential thermal energy storage materials, Sol. Energy Mater. Sol. Cells. 170 (2017) 149–159. doi:10.1016/J.SOLMAT.2017.05.036.

[13] V. Palomba, A. Frazzica, Recent advancements in sorption technology for solar thermal energy storage applications, Sol. Energy. (2018) 1–37. doi:10.1016/j.solener.2018.06.102.

[14] A. Frazzica, V. Brancato, V. Palomba, S. Vasta, Sorption Thermal Energy Storage, in: A. Frazzica, L.F. Cabeza (Eds.), Recent Adv. Mater. Syst. Therm. Energy Storage- An Introd. to Exp. Charact. Methods, Springer, 2019: pp. 33–54. doi:10.1007/978-3-319-96640-3_4.

[15] P.A.J. Donkers, L. Pel, O.C.G. Adan, Experimental studies for the cyclability of salt hydrates for thermochemical heat storage, J. Energy Storage. 5 (2016) 25–32. doi:10.1016/j.est.2015.11.005.

[16] S.K. Henninger, S.-J. Ernst, L. Gordeeva, P. Bendix, D. Fröhlich, A.D. Grekova, L. Bonaccorsi, Y. Aristov, J. Jaenchen, New materials for adsorption heat transformation and storage, Renew. Energy. 110 (2017) 59–68. doi:10.1016/j.renene.2016.08.041.

[17] M. Karthik, A. Faik, B. D'Aguanno, Graphite foam as interpenetrating matrices for phase change paraffin wax: A candidate composite for low temperature thermal energy storage, Sol. Energy Mater. Sol. Cells. 172 (2017) 324–334. doi:10.1016/J.SOLMAT.2017.08.004.

[18] O. Ola, Y. Chen, Y. Zhu, Three-dimensional carbon foam nanocomposites for thermal energy storage, Sol. Energy Mater. Sol. Cells. 191 (2019) 297–305. doi:10.1016/J.SOLMAT.2018.11.037.

[19] S. Hongois, F. Kuznik, P. Stevens, J.J. Roux, Development and characterisation of a new MgSO4-zeolite composite for long-term thermal energy storage, Sol. Energy Mater. Sol. Cells. 95 (2011) 1831–1837. doi:10.1016/j.solmat.2011.01.050.

[20] G.T. Whiting, D. Grondin, D. Stosic, S. Bennici, A. Auroux, Zeolite-MgCl2 composites as potential long-term heat storage materials: Influence of zeolite properties on heats of water sorption, Sol. Energy Mater. Sol. Cells. 128 (2014) 289–295. doi:10.1016/j.solmat.2014.05.016.

[21] K. Posern, C. Kaps, Calorimetric studies of thermochemical heat storage materials based on mixtures of MgSO4 and MgCl2, Thermochim. Acta. 502 (2010) 73–76. doi:10.1016/j.tca.2010.02.009.

[22] A. Jabbari-Hichri, S. Bennici, A. Auroux, CaCl2-containing composites as thermochemical heat storage materials, Sol. Energy Mater. Sol. Cells. 172 (2017) 177–185. doi:10.1016/J.SOLMAT.2017.07.037.

[23] C. Xu, Z. Yu, Y. Xie, Y. Ren, F. Ye, X. Ju, Study of the hydration behavior of zeolite-MgSO4 composites for long-term heat storage, Appl. Therm. Eng. 129 (2018) 250–259. doi:10.1016/J.APPLTHERMALENG.2017.10.031.

[24] S.Z. Xu, R.Z. Wang, L.W. Wang, J. Zhu, Performance characterizations and thermodynamic analysis of magnesium sulfate-impregnated zeolite 13X and activated alumina composite sorbents for thermal energy storage, Energy. 167 (2019) 889–901. doi:10.1016/J.ENERGY.2018.10.200.

[25] A. Mehrabadi, M. Farid, New salt hydrate composite for low-grade thermal energy storage, Energy. 164 (2018) 194–203. doi:10.1016/J.ENERGY.2018.08.192.

[26] T. Yan, C.Y. Wang, D. Li, Performance analysis of a solid-gas thermochemical composite sorption system for thermal energy storage and energy upgrade, Appl. Therm. Eng. 150 (2019) 512–521. doi:10.1016/J.APPLTHERMALENG.2019.01.004.

[27] Shui Wai Lin and Salvador Valera Lamas, Air Dehydration by Permeation Through Dimethylpolysiloxane/polysulfone Membrane, J. Mex. Chem. Soc. 55 (2011) 42–50.

[28] V. Brancato, L. Calabrese, V. Palomba, A. Frazzica, M. Fullana-Puig, A. Solé, L.F. Cabeza, MgSO4·7H2O filled macro cellular foams: An innovative composite sorbent for thermo-chemical energy storage applications for solar buildings, Sol. Energy. 173 (2018) 1278–1286. doi:10.1016/J.SOLENER.2018.08.075.

[29] L. Calabrese, L. Bonaccorsi, P. Bruzzaniti, G. Gullì, A. Freni, E. Proverbio, Zeolite filled siloxane composite foams: Compression property, J. Appl. Polym. Sci. (2017). doi:10.1002/app.46145.

[30] L. Calabrese, V. Brancato, V. Palomba, A. Frazzica, L.F. Cabeza, Assessment of the hydration/dehydration behaviour of MgSO4·7H2O filled cellular foams for sorption storage applications through morphological and thermo-gravimetric analyses, Sustain. Mater. Technol. 17 (2018) e00073. doi:10.1016/J.SUSMAT.2018.E00073.

[31] L. Calabrese, L. Bonaccorsi, A. Freni, E. Proverbio, Synthesis of SAPO-34 zeolite filled macrocellular foams for adsorption heat pump applications: A preliminary study, Appl. Therm. Eng. 124 (2017) 1312–1318. doi:10.1016/j.applthermaleng.2017.06.121.

[32] L. Calabrese, L. Bonaccorsi, A. Freni, E. Proverbio, Silicone composite foams for adsorption heat pump applications, Sustain. Mater. Technol. 12 (2017) 27–34. doi:10.1016/j.susmat.2017.04.002.

[33] A. Frazzica, A. Sapienza, A. Freni, Novel experimental methodology for the characterization of thermodynamic performance of advanced working pairs for adsorptive heat transformers, Appl. Therm. Eng. 72 (2014) 229–236. doi:10.1016/j.applthermaleng.2014.07.005.

[34] L. Calabrese, L. Bonaccorsi, P. Bruzzaniti, A. Freni, E. Proverbio, Morphological and functional aspects of zeolite filled siloxane composite foams, J. Appl. Polym. Sci. 135 (2018). doi:10.1002/app.45683.

[35] V.M. van Essen, H.A. Zondag, J.C. Gores, L.P.J. Bleijendaal, M. Bakker, R. Schuitema, W.G.J. van Helden, Z. He, C.C.M. Rindt, Characterization of MgSO4 Hydrate for Thermochemical Seasonal Heat Storage, J. Sol. Energy Eng. 131 (2009) 041014. doi:10.1115/1.4000275.

[36] C. Bales, P. Gantenbein, D. Jaehnig, H. Kerskes, M. Van Essen, R. Weber, H. Zondag, 031 - Chemical and Sorption Storage – Results from IEA-SHC Task 32, Eurosun 2008. (2008) 1–8.